

Magnon BEC in superfluid $^3\text{He-A}$

Yu.M. Bunkov ^{#1)} and G.E. Volovik ^{*+†}

[#] MCBT, Institut Neel, CNRS/UJF, Grenoble, 38042, France

^{*} Low Temperature Laboratory, Helsinki University of Technology, P.O.Box 5100, FIN-02015, HUT, Finland

[†] Landau Institute for Theoretical Physics RAS, Kosyginia 2, 119334 Moscow, Russia

Submitted March 2009

The new mode of magnetization precession in superfluid $^3\text{He-A}$ in a squeezed aerogel has been recently reported. We consider this mode in terms of the Bose-Einstein condensation (BEC) of magnons. The difference between magnon BEC states in $^3\text{He-A}$ and in $^3\text{He-B}$ is discussed.

PACS:

The discovery [1] and detailed investigations of the phase-coherent precession of magnetization in superfluid $^3\text{He-B}$ generated a search for similar phenomena in other systems. Superfluid $^3\text{He-A}$ could be a proper system. However, it was found that under typical conditions the coherent precession in $^3\text{He-A}$ is unstable [2] because of the convex shape of spin-orbit energy potential as function of magnetization [3, 4]. It was suggested that the shape of potential can be inverted and thus the coherent precession can be stabilized if the orbital momentum of Cooper pairs in $^3\text{He-A}$ is oriented along the applied magnetic field [5]. Recently such orientation has been reached for $^3\text{He-A}$ immersed in the axially squeezed aerogel [6], and the first experiments with the coherently precessed state (CPS) of magnetization have been reported [7]. Here we discuss the phenomenon of the coherent precession of magnetization in superfluid $^3\text{He-A}$ in terms of the Bose-Einstein condensation (BEC) of magnons, and consider the difference between magnon BEC states in $^3\text{He-A}$ (CPS) and in $^3\text{He-B}$ (HPD).

BEC is one of the most remarkable quantum phenomena. It corresponds to formation of collective quantum state, in which the macroscopic number of particles is governed by a single wave function. The formation of Bose-Einstein condensate was predicted by Einstein in 1925, for review see e.g. [8]. The almost perfect BEC state was observed in ultra cold atomic gases. In Bose liquids, the BEC is strongly modified by interactions, but still remains the key mechanism for formation of coherent quantum state, which experiences the phenomenon of superfluidity: nondissipative superfluid current. In liquid ^4He the depletion of the condensate is very large: in the limit of zero temperature only about 10% of particles occupy the state with zero momentum. Nevertheless the whole liquid (100% of atoms) forms the

coherent quantum state at $T = 0$, so that the superfluid density equals the total density, $\rho_s(T = 0) = \rho$. The latter is valid for any monoatomic superfluid system with translational invariance, including superfluid ^3He with the non BEC mechanism of coherent quantum state. If translational invariance is violated by impurities, crystal fields or other inhomogeneity, the superfluid component is suppressed: $\rho_s(T = 0) < \rho$.

Superfluidity is a very general quantum property of matter at low temperatures, with variety of possible nondissipative superfluid currents, such as supercurrent of electric charge in superconductors; hypercharge supercurrent in the vacuum of Standard Model; supercurrent of color charge in a dense quark matter; etc. The origin of superfluidity is the spontaneous violation of the $U(1)$ symmetry related to the conservation of the corresponding charge or particle number. That is why, strictly speaking, the theory of superfluidity is applicable to systems with conserved charge or particle number. However, it can be extended to systems with a weakly violated conservation law. This means that a system of sufficiently long-lived quasiparticles, such as phonons, rotons, spin waves (magnons), excitons, etc., can also form the coherent state, which is close to thermodynamic equilibrium state of Bose condensate.

The phase-coherent precession of magnetization in superfluid $^3\text{He-B}$ discovered in 1984 [1] can be considered as a realization of superfluidity of quasiparticles, which results from the BEC of magnon quasiparticles [9, 10]. In $^3\text{He-B}$, the magnon BEC is represented by a domain with a fully phase-coherent precession of magnetization, known as the Homogeneously Precessing Domain (HPD). HPD exhibits all the properties of spin superfluidity (see Reviews [10, 11, 12]). These include in particular: spin supercurrent which transports the magnetization; spin current Josephson effect and phase-slip processes at the critical current; and spin current vor-

¹⁾yuriy.bunkov@grenoble.cnrs.fr; volovik@boojum.hut.fi

tex – a topological defect which is the analog of a quantized vortex in superfluids and of an Abrikosov vortex in superconductors; etc. The temperature at which the BEC in $^3\text{He-B}$ exists is by several orders of magnitude smaller than the transition temperature of magnon Bose condensation [10]. This implies that the gas of magnons forms practically 100% BEC state, even if only a small number of excitations is originally pumped into the $^3\text{He-B}$ sample. Magnon condensation to the lowest energy states has been also found in yttrium-iron garnet [13, 14] with the fraction of the condensed magnons being less than 1%. Condensation of such quasiparticles as polaritons to the lowest energy states has been reported in Refs. [15, 16]. The polariton condensate is formed as dynamical out-of-equilibrium state, which is rather far from the true thermodynamic BEC.

In bulk $^3\text{He-A}$, the BEC of magnons is unstable because of attractive interaction between magnons, which is reflected in the concave shape of the spin-orbit (dipole-dipole) interaction potential. However, under special conditions, when $^3\text{He-A}$ is confined in the properly deformed aerogel, interaction between magnons becomes repulsive and a stable Bose condensate is formed. The magnon BEC is described in terms of complex order parameter Ψ , which is related to the precessing spin in the following way [10, 11]:

$$\Psi = \sqrt{2S/\hbar} \sin \frac{\beta}{2} e^{i\omega t+i\alpha}, \quad (1)$$

$$S_x + iS_y = S \sin \beta e^{i\omega t+i\alpha}, \quad (2)$$

$$N_M = \int d^3r |\Psi|^2 = \int d^3r \frac{S - S_z}{\hbar}. \quad (3)$$

Here $\mathbf{S} = (S_x, S_y, S_z = S \cos \beta)$ is the vector of spin density; β is the tipping angle of precessing magnetization; ω is the precession frequency (in the regime of continuous NMR, it is the frequency ω_{RF} of the applied RF field and it plays the role of the chemical potential $\mu = \omega$ for magnons); α is the phase of precession; S is the equilibrium value of spin density in the applied magnetic field $\mathbf{H} = H\hat{\mathbf{z}}$ (in ^3He liquids $S = \chi H/\gamma$, where χ is spin susceptibility of $^3\text{He-B}$ or $^3\text{He-A}$, and γ the gyromagnetic ratio of the ^3He atom); $|\Psi|^2 = n_M$ is the density of magnons and N_M is the total number of magnons in the precessing state.

The corresponding Gross-Pitaevskii equation is

$$\frac{\delta F}{\delta \Psi^*} = 0, \quad (4)$$

$$F = \int d^3r \left(\frac{|\nabla \Psi|^2}{2m_M} + (\omega_L(\mathbf{r}) - \omega)|\Psi|^2 + F_D \right). \quad (5)$$

Here $\omega_L(\mathbf{r}) = \gamma H(\mathbf{r})$ is the local Larmor frequency which plays the role of external potential for magnons;

m_M is the magnon mass; and F_D is the spin-orbit interaction averaged over the fast precession, which plays the part of interaction between magnons. In superfluid ^3He , F_D depends on interaction between spin and orbital degrees of freedom and is determined by the direction $\hat{\mathbf{l}}$ of the orbital angular momentum of Cooper pairs. For $^3\text{He-A}$, it has the form [5]

$$F_D = \frac{\chi \Omega_L^2}{4} \times \left[-2 \frac{|\Psi|^2}{S} + \frac{|\Psi|^4}{S^2} + \left(-2 + 4 \frac{|\Psi|^2}{S} - \frac{7}{4} \frac{|\Psi|^4}{S^2} \right) \sin^2 \beta_L \right], \quad (6)$$

where β_L is the angle of $\hat{\mathbf{l}}$ with respect to magnetic field; and $\Omega_L \ll \omega_L$ is the Leggett frequency characterizing the spin-orbit coupling (we put $\hbar = \gamma = 1$).

While the sign of the quadratic term in Eq.(6) is not important because it only leads to the shift of the chemical potential $\mu \equiv \omega$ in Eq.(5), the sign of quartic term is crucial for stability of BEC. In a static bulk $^3\text{He-A}$, when $\Psi = 0$, the spin-orbit energy F_D in Eq.(6) is minimized when $\hat{\mathbf{l}}$ is perpendicular to magnetic field, $\sin \beta_L = 1$. Then one has

$$F_D = \frac{\chi \Omega_L^2}{4} \left[-2 + 2 \frac{|\Psi|^2}{S} - \frac{3}{4} \frac{|\Psi|^4}{S^2} \right], \quad (7)$$

with the negative quartic term. The attractive interaction between magnons destabilizes the BEC, which means that homogeneous precession of magnetization in $^3\text{He-A}$ becomes unstable, as was predicted by Fomin [3] and observed experimentally in Kapitza Institute [2].

However, as follows from (6), at sufficiently large magnon density $n_M = |\Psi|^2$

$$\frac{8 + \sqrt{8}}{7} S > n_M > \frac{8 - \sqrt{8}}{7} S, \quad (8)$$

the factor in front of $\sin^2 \beta_L$ becomes positive. Therefore it becomes energetically favorable to orient the orbital momentum along the magnetic field, $\beta_L = 0$, and after that the quartic term in Eq.(6) becomes positive. In other words, with increasing the density of Bose condensate, the originally attractive interaction between bosons should spontaneously become repulsive when the critical magnon density $n_M = S(8 - \sqrt{8})/7$ is reached. If this happens, the magnon BEC becomes stable and in this way the state with coherent precession (CPS) could be formed [5]. This self-stabilization effect is similar to the effect of Q -ball, where bosons create the potential well in which they condense (on theory and experiment of magnon condensation into Q -ball see Ref. [17]). However, such a self-sustaining BEC with originally attractive boson interaction has not been achieved

experimentally in bulk $^3\text{He-A}$, most probably because of the large dissipation, due to which the threshold value of the condensate density has not been reached. Finally the fixed orientation of $\hat{\mathbf{l}}$ has been achieved in $^3\text{He-A}$ confined in aerogel – the material with high porosity, which is about 98% of volume in our experiments. As a consequence, when magnetic field was oriented along $\hat{\mathbf{l}}$ (i.e. in geometry with $\beta_L = 0$), the first indication of coherent precession in $^3\text{He-A}$ has been reported [7].

Silicon strands of aerogel play the role of impurities with local anisotropy along the strands. According to the Larkin-Imry-Ma effect, the random anisotropy suppresses the orientational long-range order of the orbital vector $\hat{\mathbf{l}}$; however, when the aerogel sample is deformed the long-range order of $\hat{\mathbf{l}}$ is restored [18]. Experiments with globally squeezed aerogel [6] demonstrated that a uni-axial deformation by about 1% is sufficient for global orientation of the vector $\hat{\mathbf{l}}$ along \mathbf{H} : the observed shape of the NMR line has a large negative frequency shift corresponding to β_L spreading from 0 to about 20° . Previously the small negative frequency shift has been observed in some samples of aerogel [19, 20], which can be explained by a residual deformations of these samples.

Let us first consider a perfect aerogel sample with global orientation of the vector $\hat{\mathbf{l}}$ along \mathbf{H} . For $\beta_L = 0$, the GL free energy acquires the standard form:

$$F = \int d^3r \left(\frac{|\nabla\Psi|^2}{2m_M} + (\omega_L(\mathbf{r}) - \mu)|\Psi|^2 + \frac{1}{2}b|\Psi|^4 \right), \quad (9)$$

where we modified the chemical potential by the constant frequency shift:

$$\mu = \omega + \frac{\Omega_L^2}{2\omega}, \quad (10)$$

and the parameter b of repulsive magnon interaction is

$$b = \frac{\Omega_L^2}{2\omega S} \quad (11)$$

At $\mu > \omega_L$, magnon BEC must be formed with density

$$|\Psi|^2 = \frac{\mu - \omega_L}{b}. \quad (12)$$

This corresponds to the following dependence of the frequency shift on tipping angle β of coherence precession:

$$\omega - \omega_L = -\frac{\Omega_L^2}{2\omega} \cos\beta. \quad (13)$$

If the precession is induced by continuous wave (CW) NMR, one should also add the interaction with the RF field, \mathbf{H}_{RF} , which is transverse to the applied constant field \mathbf{H} . In CW NMR experiments, the RF field prescribes the frequency of precession, $\omega = \omega_{\text{RF}}$, and thus

fixes the chemical potential μ . In the precession frame, where both the RF field and the spin density \mathbf{S} are constant in time, the interaction term is

$$F_{\text{RF}} = -\gamma \mathbf{H}_{\text{RF}} \cdot \mathbf{S} = -\gamma H_{\text{RF}} S_{\perp} \cos(\alpha - \alpha_{\text{RF}}), \quad (14)$$

where H_{RF} and α_{RF} are the amplitude and the phase of the RF field. In the language of magnon BEC, this term softly breaks the $U(1)$ -symmetry and serves as a source of magnons [21]:

$$F_{\text{RF}}(\psi) = -\frac{1}{2}\eta(\psi + \psi^*), \quad (15)$$

which compensates the loss of magnons due to magnetic relaxation. The symmetry-breaking field η is:

$$\eta = \gamma H_{\text{RF}} \sqrt{2S - n_M}. \quad (16)$$

The phase difference between the condensate and the RF field, $\alpha - \alpha_{\text{RF}}$, is determined by the energy losses due to magnetic relaxation, which is compensated by the pumping of power from the CW RF field:

$$W_+ = \omega S H_{\text{RF}} \sin\beta \sin(\alpha - \alpha_{\text{RF}}). \quad (17)$$

The phase shift is automatically adjusted to compensate the losses. If dissipation is small, the phase shift is small, $\alpha - \alpha_{\text{RF}} \ll 1$, and can be neglected. The neglected quadratic term $(\alpha - \alpha_{\text{RF}})^2$ leads to the nonzero mass of the Goldstone boson – quantum of sound waves (phonon) in the magnon superfluid [21]; in $^3\text{He-B}$ the phonon mass, which is proportional to $\sqrt{H_{\text{RF}}}$, has been measured [22, 23]. In the limit of small dissipation the main role of the RF field is to modify the profile of the GL free energy in (9) by adding the term:

$$F_{\text{RF}}(n_M) = -\eta|\psi| = -\gamma H_{\text{RF}} \sqrt{n_M(2S - n_M)}. \quad (18)$$

Equation $dF/dn_M = 0$ now gives the following modification of Eq.(13) for NMR frequency shift as function of magnon density $n_M = |\Psi|^2 = S(1 - \cos\beta)$:

$$\omega - \omega_L = -\frac{\Omega_L^2}{2\omega_L} \cos\beta - \gamma H_{\text{RF}} \cot\beta. \quad (19)$$

For finite $\alpha - \alpha_{\text{RF}}$, the last term should be multiplied by $\cos(\alpha - \alpha_{\text{RF}})$. According to Ref. [7], the energy losses are proportional to square of transverse magnetization, and thus we have:

$$W_- = \sigma \sin^2\beta, \quad (20)$$

where σ is the phenomenological parameter.

Since the pumping (17) is proportional to $\sin\beta \sin(\alpha - \alpha_{\text{RF}})$, then there must be a critical tipping

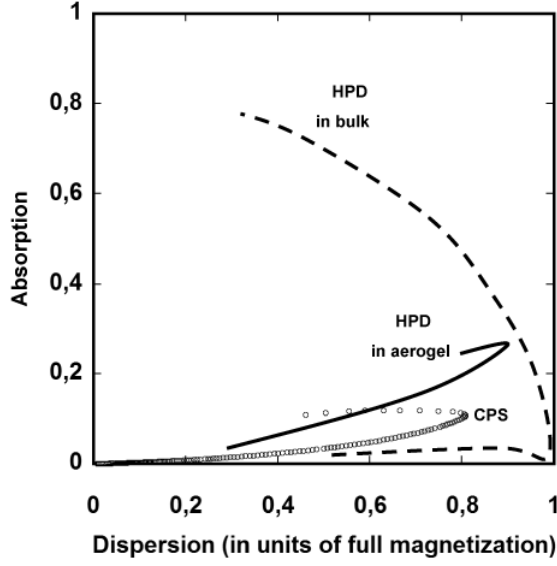


Fig. 1. Typical absorption/dispersion relation for different states of coherent precession. HPD in the bulk $^3\text{He-B}$ is shown schematically. Signals from HPD in $^3\text{He-B}$ in aerogel and from the CPS state in $^3\text{He-A}$ in aerogel correspond to experimental data in Ref. [7].

angle β_c , at which the pumping cannot compensate the losses, $\sin \beta_c = \omega S H_{RF} / \sigma$, and the coherent precession collapses. For a homogeneous case the critical angle should correspond to $\alpha_c = \alpha - \alpha_{RF} = 90^\circ$. For the real case, it is instructive to consider the phase portrait of the CW NMR signal measured in experiments: the time development of the signal in the plane of absorption $M_\perp \sin(\alpha - \alpha_{RF})$ and dispersion $M_\perp \cos(\alpha - \alpha_{RF})$, where M_\perp is the total transverse magnetization in the cell. This diagram demonstrates the time dependence of angle $\alpha - \alpha_{RF}$ during sweeping the frequency shift $\omega - \omega_L$ (actually the field H is swept). For the HPD state in bulk $^3\text{He-B}$ this is shown by dashed line in Fig.1. At first stage the precessing domain is filling the cell. During the process of filling the absorption remains rather small, and thus dispersion corresponds to the full transverse magnetization M_\perp which grows linearly with growing domain. After domain fills the whole cell, the full transverse magnetization is fixed, and the signal follows the circle around the origin. This corresponds to increase of angle $\alpha - \alpha_{RF}$ due to increasing of relaxation. Finally the coherent precession collapses. The critical angle α_c for HPD is typically about $70^\circ - 45^\circ$. It is significantly smaller than expected 90° , and it is due to inhomogeneity of relaxation. In the region of larger magnetic (Leggett-Takagi) relaxation, the local $\alpha(\mathbf{r}) - \alpha_{RF}$ is larger.

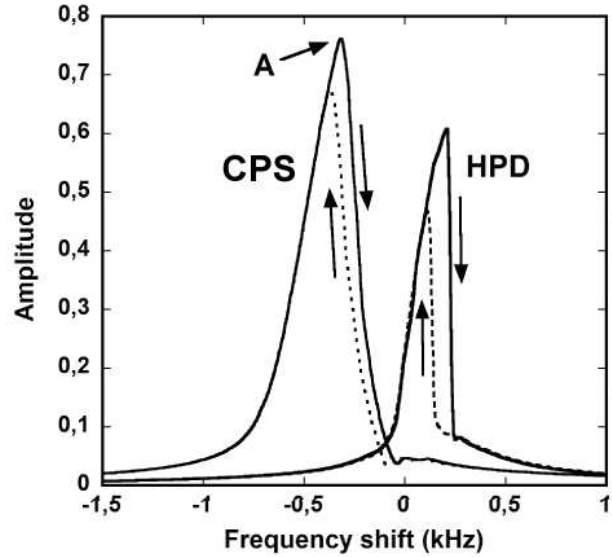


Fig. 2. Formation of the homogeneously precessing domain (HPD) in $^3\text{He-B}$ and of phase-coherent precession (CPS) in $^3\text{He-A}$ under upward and downward frequency sweeps. The experimental data are from [7].

The spatial gradient of angle α generates the spin supercurrent, which transports the magnetization and supports the coherence of precession. The HPD state collapses, when the local angle of precession reaches the 90° in some region of the cell.

A similar behavior was found both for HPD and CPS states in aerogel, as shown in Fig.1. But there is also a peculiar difference which is related to a spatial inhomogeneity of the aerogel sample. The first HPD in $^3\text{He-B}$ in aerogel was observed on a very inhomogeneous sample. As a result, the HPD was created locally and was not able to grow through the whole sample [24]. Later on this experiment was repeated with the more homogeneous aerogel [25], and HPD filled the whole sample. Indeed, the aerogel samples of such quality are very rare.

The sample of aerogel, used in the work [7], can be considered as of intermediate quality. The HPD signal can be created in the whole cell, but the absorption signal is rather big. The spatial inhomogeneity of absorption is also clear from a small value of threshold α_c , at which collapse occurs: it is about 15° in Fig. 1. The threshold $\sin \beta_c$ was found to increase with increasing H_{RF} (see Fig.3 in Ref. [7]), and the precession with large β was finally achieved at large H_{RF} . At small β the influence of the diverging $H_{RF} \cot \beta$ term in (19) is clearly seen, while at large β , signals at different excitations fall onto a universal curve independent of the amplitude of the RF-field, as shown in the Fig. 3 of

Ref. [7]. This demonstrates that at large β the magnon BEC is self-consistent and is not sensitive to the RF-field; the latter is only needed for compensation of the spin and energy losses. The amplitude of highest RF field, used in the experiments of Ref.[7] was only 0.05 Oe, which is much smaller than the frequency shift and the inhomogeneity of the NMR line.

What can be origin of the spatial inhomogeneity of relaxation? The candidates for regions with high dissipation could be topological defects, such as solitons – domain walls between two possible orientations of vector $\hat{\mathbf{l}}$ in the deformed aerogel: parallel and anti-parallel to \mathbf{H} . If the density of solitons is relatively small, and thus the regions with small dissipation are dominating, the observed average value $\langle \sin(\alpha(\mathbf{r}) - \alpha_{\text{RF}}) \rangle$ will be small. In Fig. 2 we reproduce the signals from Ref.[7]. The important difference between the CPS and HPD signals, observed in aerogel, and the HPD signal in bulk is the fact that after collapse the states in aerogel are not destroyed completely: the coherent precession survives in some parts of the sample. Furthermore, the state can be excited by sweeping the frequency back. The latter shows, that there are some regions in the sample with a very different orientation of the order parameter, which can get the energy from the RF field, transport magnetization by spin supercurrents to the other parts of the cell and restore the CPS in the whole cell. This is a natural explanation, whose justification however requires the detailed knowledge of the distribution of inhomogeneity and texture of the order parameter in aerogel.

Of course, the final proof of the coherence of precession in $^3\text{He-A}$ in aerogel would be the observation of the free precession after a pulsed NMR or after a switch off the CW NMR. However, it is not excluded that what was observed in Ref.[7] corresponds not to a single domain of precession, but to a few weakly interacting CPS domains, which are kept in phase by the RF field rather than by supercurrents between them. In this case it would not be so easy to detect the coherent precession in the pulsed NMR. Example of such kind is provided by experiments with bulk $^3\text{He-B}$, which was divided into 5 independent parts by mylar foils [26]. Then in the CW NMR the signal corresponded to all 5 HPD states being in phase, while in pulsed NMR the coherence between the HPD state was lost and beating of 5 independent HPD states was observed.

In conclusion, in contrast to the homogeneously precessing domain (HPD) in $^3\text{He-B}$, the magnon Bose condensation in $^3\text{He-A}$ obeys the standard Gross-Pitaevskii equation. In bulk $^3\text{He-A}$, the Bose condensate of magnons is unstable because of the attractive interaction between magnons. In $^3\text{He-A}$ confined in aerogel,

the repulsive interaction is achieved by the proper deformation of the aerogel sample, and the Bose condensate becomes stable. The magnon BEC in $^3\text{He-A}$ adds to the other two coherent states of magnons observed in $^3\text{He-B}$: HPD state and Q -ball [17]. New experiments to observe the superfluid phenomena accompanying the coherent precession in $^3\text{He-A}$ (spin supercurrent transport of magnetization, Josephson phenomena and spin-current vortices) are expected in future. It would be interesting to search for similar dynamical coherent states of excitations in other condensed matter systems (see for example Refs. [13, 14, 15, 16]).

ACKNOWLEDGMENTS

This work was supported by the program ULTI of the European Union (contract number: RITA-CT-2003-505313) and the project of collaboration between of CNRS and Russian Academy of science No 21253. GEV is supported in part by the Russian Foundation for Basic Research (grant 06-02-16002-a) and the Khalatnikov–Starobinsky leading scientific school (grant 4899.2008.2)

1. A.S. Borovik-Romanov, Yu.M. Bunkov, V.V. Dmitriev, *et al.*, JETP Lett. **40**, 1033, (1984); I.A. Fomin, JETP Lett. **40**, 1036 (1984).
2. A.S. Borovik-Romanov, Yu.M. Bunkov, V.V. Dmitriev, *et al.*, JETP Lett. **39**, 469–473 (1984).
3. I.A. Fomin, JETP Lett. **30**, 164–166 (1979).
4. I.A. Fomin, JETP Lett. **39**, 466–469 (1984).
5. Yu. M. Bunkov and G. E. Volovik, Europhys. Lett. **21**, 837–843 (1993).
6. T. Kunimatsu, T. Sato, K. Izumina, *et al.*, JETP Lett. **86**, 216 (2007).
7. T. Sato, T. Kunimatsu, K. Izumina, *et al.* Phys. Rev. Lett. **101**, 055301 (2008).
8. F. Dalfovo, S. Giorgini, L.P. Pitaevskii, *et al.*, Rev. Mod. Phys. **71**, 463–512 (1999); S. Giorgini, L.P. Pitaevskii and S. Stringari, Rev. Mod. Phys. **80**, 1215–1274 (2008).
9. Yu.M. Bunkov and G.E. Volovik, J. Low Temp. Phys. **150**, 135–144 (2008).
10. G.E. Volovik, J. Low Temp. Phys. **153**, 266–284 (2008).
11. I.A. Fomin, Physica **B 169**, 153 (1991).
12. Yu.M. Bunkov, J. Low Temp. Phys. **135**, 337 (2004); in: Prog. Low Temp. Phys., Halperin, Elsevier, **14**, p. 69 (1995).
13. S.O. Demokritov, V.E. Demidov, O. Dzyapko, *et al.*, Nature **443**, 430 (2006).
14. V.E. Demidov, O. Dzyapko, S.O. Demokritov, *et al.*, Phys. Rev. Lett. **100**, 047205 (2008).
15. J. Kasprzak, M. Richard, S. Kundermann, *et al.*, Nature **443**, 409 (2006).

16. J. Kasprzak, M. Richard, R. Andre and Le Si Dang, J. Europ. Opt. Soc. - Rapid Publications **3**, 08023 (2008).
17. Yu.M. Bunkov and G.E. Volovik, Phys. Rev. Lett. **98**, 265302 (2007).
18. G.E. Volovik, JETP Lett. **84**, 455 (2006).
19. B.I. Barker, Y. Lee, L. Polukhina, *et al.*, Phys. Rev. Lett. **85**, 2148 (2000).
20. V.V. Dmitriev, L.V. Levitin, N. Mulders *et al.*, JETP Lett. **84**, 461 (2006).
21. G.E. Volovik, JETP Lett. **87**, 639–640 (2008).
22. V.V. Dmitriev, V.V. Zavjalov and D.Ye. Zmeev, J. Low Temp. Phys. **138**, 765–770 (2005).
23. M. Človečko, E. Gažo, M. Kupka *et al.*, Phys. Rev. Lett. **100**, 155301 (2008).
24. Yu.M. Bunkov, E. Collin, H. Godfrin *et al.*, Physica **B 329**, 305 (2003).
25. V.V. Dmitriev, V.V. Zavjalov, D.E. Zmeev et al., JETP Lett. **76**, 312–317 (2002).
26. A.S. Borovik-Romanov, Yu.M. Bunkov, V.V. Dmitriev *et al.*, Sov. Phys. JETP, **61**, 1199 (1985).